

# On the Design of Multidimensional Signal Sets for OFDM Systems

Dennis L. Goeckel and Ganesh Ananthaswamy

**Abstract**—An orthogonal frequency division multiplexing (OFDM) system operating over a wireless communication channel effectively forms a number of parallel frequency-nonspecific fading channels, thereby obviating the need for complex equalization and thus greatly simplifying equalization/decoding. However, the OFDM system also exhibits two weaknesses relative to its single-carrier counterparts: 1) the diversity achieved by the OFDM system can be less than a single-carrier system employing the same error control code in a signaling environment rich in diversity and 2) the baseband transmitted signal can exhibit significant amplitude fluctuation over time, thereby precluding efficient transmit amplifier operation. In this paper, nonstandard multidimensional signal sets matched to the OFDM framework are prescribed that address both of these issues. The proposed signal sets are chosen to maximize the diversity achieved by an uncoded system under a constraint to control the peak-to-mean envelope power ratio (PMEPR) of the baseband transmitted waveform. The cost of employing the proposed signal sets is an increase in decoding complexity, as essentially a small amount of controlled equalization has been added to the receiver; thus, the resulting system can be viewed as a hybrid between an OFDM system and a standard single-carrier system. Numerical results are presented which suggest that: 1) the system can provide an attractive alternative to a standard OFDM system in terms of required average transmitted SNR versus receiver complexity and 2) the system yields a modest reduction in PMEPR versus a standard OFDM system.

**Index Terms**—Coded modulation, equalization, fading channels, orthogonal frequency division multiplexing.

## I. INTRODUCTION

A MAJOR goal of modern communications is the development of a reliable high-speed wireless communication system that supports high user mobility; however, the achievement of this goal is inhibited by multipath fading, which intro-

duces intersymbol interference (ISI) among transmitted symbols on wide-band wireless channels. Communication theory has revealed two effective methods for reliable communication in systems, either wired or wireless, subject to ISI: 1) a multicarrier system employing error control coding and 2) a single-carrier system that employs a combination of error control coding and precoding/equalization.

The time-varying nature of the multipath fading of a wireless channel in a system with highly mobile users precludes the direct application of many methods that can be applied over fixed ISI channels (e.g., Tomlinson–Harashima precoding (THP) [1], [2] or discrete multitone modulation (DMT) with adaptive bit loading [3]); in particular, outdated knowledge of the multipath fading values at the transmitter is only useful in wireless systems with limited mobility [4]. When reliable knowledge of the current multipath fading values is not available at the transmitter, coded symbols are generally interleaved before being transmitted across the channel, thereby providing code diversity. In the receiver of a single-carrier system, the required deinterleaving between the equalizer and the decoder of the error control code makes the optimal combination of these two operations prohibitively complex; instead, soft-output equalizers are often employed that provide to the decoder not only decisions on the equalized channel bits, but also soft information that characterizes the reliability of each of these bit decisions [5], [6]. Performance can then be further improved at the cost of complexity by iterating soft information between the equalizer and decoder in the “turbo” fashion [5]. One major drawback of this single-carrier architecture is that the soft-output equalizer itself can be too complex for implementation, especially in high-speed single-carrier data systems where, because of the extremely short symbol period, the significant ISI can extend over many data symbols and the receiver processing time per data symbol is severely limited.

In contrast to a single-carrier system, a key tenet of an orthogonal frequency division multiplexing (OFDM) system operating on a wireless communication channel is that the fading affecting each coded symbol is frequency-nonspecific, thereby making equalization trivial and allowing optimal combined equalization/decoding of reasonable complexity. However, this comes at a performance cost; if both systems employ the same error control code and *perfect* interleaving of the coded symbols is assumed, a coded multicarrier system achieves significantly less diversity than a coded single-carrier system on a frequency-selective fading channel (see [7, Ch. 6]). The reason for this limitation of the OFDM system is as follows. Because the effective discrete-time channel between the encoder and the decoder in

Paper approved by C. Tellambura, the Editor for Modulation and Signal Design of the IEEE Communications Society. Manuscript received March 16, 2000; revised March 1, 2001, and August 14, 2001. This paper was supported in part by the National Science Foundation under Grant NCR-9714597 and CAREER Award CCR-9875482. This paper was presented in part at the Thirty-Sixth Annual Allerton Conference on Communication, Control, and Computing, Monticello, IL, September 1998, at the 1999 International Conference on Communications, Vancouver, British Columbia, Canada, June 1999, and at the 1999 IEEE Wireless Communications and Networking Conference, New Orleans, LA, September 1999.

D. L. Goeckel is with the Electrical and Computer Engineering Department, University of Massachusetts, Amherst, MA 01003-5110 USA (e-mail: goeckel@ecs.umass.edu).

G. Ananthaswamy was with the Electrical and Computer Engineering Department, University of Massachusetts, Amherst, MA 01003-5110 USA. He is now with Analog Devices, Inc., Wilmington, MA 01887 USA (e-mail: ganesh.ananthaswamy@analog.com).

Publisher Item Identifier S 0090-6778(02)02021-4.

an OFDM system operating on a Rayleigh fading ISI channel is identical to the effective channel obtained in a frequency-nonselective Rayleigh fading channel, the achievable diversity in an OFDM system is upper bounded by the minimum Hamming distance of the error control code employed, whereas the coded single-carrier system can achieve diversity equal to the product of the frequency diversity available on the channel and the minimum Hamming distance of the error control code. Thus, if a system is operating in an environment rich in diversity over the allowable delay-bandwidth of a codeword, the single-carrier system can greatly outperform the OFDM system. Furthermore, because the OFDM signal is effectively constructed in the frequency domain, the transmitted signal can exhibit a large peak-to-mean envelope power ratio (PMEPR), thus precluding efficient operation of the amplifier in the transmitter [8].

In this paper, a coded modulation technique is proposed that draws symbols from a signal set in multiple complex dimensions; each complex dimension of the selected symbol is then placed on a properly chosen subcarrier of the OFDM system. Under a constraint to help control the PMEPR of the baseband transmitted signal, the goal in the design of these multidimensional signal sets is to maximize the diversity achieved by an uncoded system. This goal is similar to that of the work in [9], [10], where the target application was single-carrier systems on frequency-nonselective fading channels. However, in contrast to the work in [9] and [10], where the multidimensional signal sets increase the amplifier linearity requirements of a single-carrier system, the signal sets proposed in this paper are subject to an extra constraint to help control the PMEPR of the OFDM system, thus modestly reducing the linearity requirements of the transmit amplifier in the OFDM system. In addition, the natural consideration of coding across these multidimensional signal sets is addressed, which motivates the important consideration of the optimal combination of coding and modulation to minimize receiver complexity, which will have a significant bearing on the utility of the work in [9] and [10].

In Section II, both the constraint for PMEPR control and the selection of the subcarriers on which to place the complex dimensions of a symbol drawn from the multidimensional signal set arise naturally from a consideration of the inverse fast Fourier transform (IFFT) that is at the center of the OFDM transmitter. In Section III, numerical results are presented for the application of the signal sets in both uncoded and coded systems in terms of average received SNR. Section IV presents a PMEPR characterization of the resulting system. Finally, Section V presents the conclusions.

## II. MULTIDIMENSIONAL SIGNAL SETS

### A. OFDM System Architecture

In this section, the well-documented (e.g., see [11, Fig. 1]) OFDM system architecture is briefly described to establish appropriate notation. Consider an OFDM system with  $N$  subcarriers, and let  $X_{k,i}$  be the  $k$ th symbol to be placed on subcarrier  $i$ ,  $0 \leq i \leq N-1$ , during time  $kT_s \leq t \leq (k+1)T_s$ , where  $T_s$  is the OFDM symbol time. Letting  $\underline{X}_k = (X_{k,0}, X_{k,1}, \dots, X_{k,N-1})^T$  be the vector

of subcarrier symbols for the  $k$ th OFDM symbol, the corresponding time-domain sequence is obtained via an IFFT as

$$x_{k,l} = \frac{1}{\sqrt{N}} \sum_{i=0}^{N-1} X_{k,i} e^{j2\pi li/N}, \quad 0 \leq l \leq N-1.$$

It will be convenient to write  $\mathcal{F}_N^{-1}(\underline{X}_k) = \underline{x}_k$  and  $\mathcal{F}_N(\underline{x}_k) = \underline{X}_k$ , where  $\mathcal{F}_N$  is the energy-preserving  $N$ -point discrete Fourier transform operator, and  $\underline{x}_k = (x_{k,0}, x_{k,1}, \dots, x_{k,N-1})^T$ . After the cyclic prefix is added, the resulting samples are input to a digital-to-analog (D/A) converter, whose output is the complex envelope  $s(t)$  of the transmitted signal. The received signal will in general be given by  $r(t) = \int h(t, \tau) s(t - \tau) d\tau + n(t)$ , where  $h(t, \cdot)$  is the complex baseband representation of the channel response of the frequency-selective fading channel at time  $t$ , and  $n(t)$  is a zero-mean stationary Gaussian random process with two-sided power spectral density  $N_0/2$ . Throughout this paper, it will be assumed that the channel varies slowly enough that it can be modeled as approximately constant over the duration of an OFDM symbol; thus, the time variable of the channel will be suppressed to yield  $r(t) = \int h(\tau) s(t - \tau) d\tau + n(t)$ . Furthermore, the key assumption that effectively results in a frequency-nonselective fading channel for the coded symbols in an OFDM system will be assumed; that is, the subcarrier bandwidth ( $\approx 1/T_s$ ) is much smaller than the coherence frequency of the frequency-selective fading channel.

The received complex baseband signal  $r(t)$  is input to an analog-to-digital (A/D) converter; at the output of the A/D, the cyclic prefix is discarded, and the Fourier transform  $\underline{Y}_k = (Y_{k,0}, Y_{k,1}, \dots, Y_{k,N-1})^T$  of the  $N$ -vector of samples corresponding to the  $k$ th OFDM codeword is calculated. Assuming both that the cyclic prefix is of sufficient length and that perfect timing, carrier frequency, and carrier phase recovery is achieved, the standard ISI-free framework for OFDM coded modulation design is obtained as  $Y_{k,i} = H_{k,i} X_{k,i} + n_{k,i}$ , where  $H_{k,i}$  is the “flat” fading affecting the  $k$ th symbol of the  $i$ th subcarrier and  $n_{k,i}$  is a collection of zero-mean IID complex Gaussian random variables, each with  $E[|n_{k,i}|^2] = N_0$ . Under the Gaussian wide-sense stationary uncorrelated scattering (GWSSUS) model [12],  $H_{k,i}$  is a correlated (both across  $k$  and  $i$ ) two-dimensional (2-D) sequence of jointly Gaussian complex random variables. Because these random variables decorrelate with time separation (in the index  $k$ ) and frequency separation (in the index  $i$ ), it is desirable to spread the variation in the transmitted signal caused by a given codeword difference as broadly as possible within the allowable bandwidth–delay product of the system. In particular, frequency diversity can be exploited for a single uncoded bit if the variation in the transmitted signal caused by that bit’s value is spread as broadly as possible in the  $i$  dimension [13, p. 777].

### B. Design Criteria

To motivate the construction, consider the decimation-in-input decomposition of an 8-point IFFT into two 4-point IFFTs, as shown in Fig. 1, where  $\mathcal{F}_{N,i}^{-1}(\underline{X}_k)$  has been

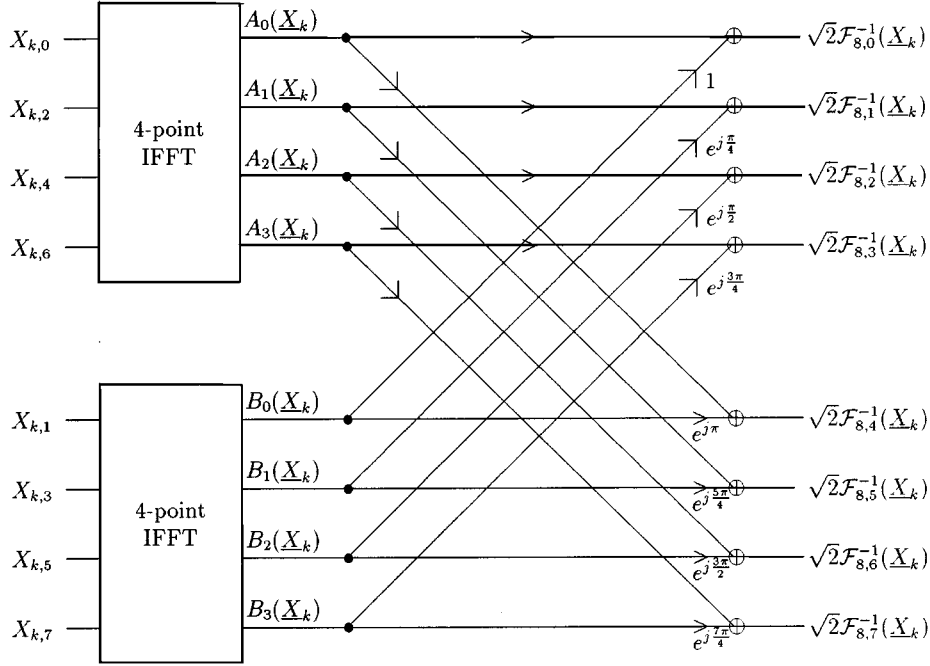


Fig. 1. The “butterfly” combining to get an 8-point IFFT from two 4-point IFFTs in a decimation-in-input scheme.

defined as the  $i$ th component of the  $N$ -point energy-preserving IFFT of  $\underline{X}_k$ . There are two key things to note: 1) since

$$|\mathcal{F}_{N,i}^{-1}(\underline{X}_k)| \leq \frac{|A_{i \bmod 4}(\underline{X}_k)|}{\sqrt{2}} + \frac{|B_{i \bmod 4}(\underline{X}_k)|}{\sqrt{2}}$$

suppressing large amplitudes in the output of the 4-point IFFTs aids in suppressing large amplitudes in the output of the 8-point IFFT, and 2) the inputs to a given 4-point IFFT are separated in frequency by two subcarriers. More generally, the inputs to a given  $M$ -point IFFT in the decomposition-in-input decomposition of an  $N$ -point IFFT in the transmitter of an OFDM system with  $N$  subcarriers will be separated by  $N/M$  subcarriers. This implies that the subcarriers corresponding to a given  $M$ -point IFFT in the decomposition are equally spaced across the bandwidth of the system, and thus an uncoded system operating on these  $M$  subcarriers with a properly chosen signal set can achieve  $M$ th-order diversity on a frequency-selective channel of minimum frequency diversity of at least  $M$ .

The two observations above motivate the following design criteria. The goal is to find a signal set  $S = \{\underline{s}_i: i = 0, \dots, K-1\}$  of  $K$  signals in  $M$  complex dimensions [i.e.,  $\underline{s}_i = (s_{i,0}, s_{i,1}, \dots, s_{i,M-1})^T$ ] such that  $\max_{\underline{s}_i \in S} \max_j |\mathcal{F}_{M,j}^{-1}(\underline{s}_i)|$  is minimized, and such that the maximum pairwise error probability between any two signals in  $S$  is as small as possible. Under the assumptions of independent Rayleigh fading in each complex dimension and a high SNR, minimizing the maximum pairwise error probability between any two signals in  $S$  can be done by maximizing the minimum pairwise product distance

$$d_{P,\min}(S) = \min_{\underline{s}_i, \underline{s}_j \in S, i \neq j} \prod_{m=0}^{M-1} |s_{i,m} - s_{j,m}|.$$

### C. Signal Set Construction

The  $M$ -fold product of a standard signal set defined in one complex dimension [e.g., binary phase-shift keying (BPSK), quadrature phase-shift keying (QPSK), or quadrature amplitude modulation (QAM)] possesses both good minimum Euclidean distance and relatively small PMEPR. Thus, consider selecting  $S$  such that the  $M$ -point IFFT of each signal point in  $S$  lies in the  $M$ -fold product  $\mathcal{Z}^M = \mathcal{Z} \times \mathcal{Z} \times \dots \times \mathcal{Z}$  of a standard signal set  $\mathcal{Z}$ ; that is,  $S = \{\mathcal{F}_M(\underline{x}): \underline{x} \in \mathcal{Z}^M\}$ . However, this selection does not maximize  $d_{P,\min}(S)$ . In fact, consider any distinct  $z_i$  and  $z_j$  in  $\mathcal{Z}$ . Then  $\underline{s}_0 \triangleq \mathcal{F}_M((z_i, z_i, \dots, z_i)^T)$  and  $\underline{s}_1 \triangleq \mathcal{F}_M((z_j, z_j, \dots, z_j)^T)$  are in  $S$ , and

$$\begin{aligned} \underline{s}_0 - \underline{s}_1 &= \mathcal{F}_M((z_i - z_j, z_i - z_j, \dots, z_i - z_j)^T) \\ &= \left( \sqrt{M}(z_i - z_j), 0, 0, \dots, 0 \right)^T \end{aligned}$$

and thus  $d_{P,\min}(S) = 0$ . Note that having a product distance equal to zero does not imply that the signal set is useless—it only indicates that the signal set does not have full diversity  $M$  and thus is less desirable at high SNRs than a signal set that has nonzero product distance.

This motivates the following modification, which can be viewed as a constrained version of the work in [10]:  $S$  is selected such that the  $M$ -point IFFT of each of the signals in  $S$  lies in  $e^{j\phi_0}\mathcal{Z} \times e^{j\phi_1}\mathcal{Z} \times \dots \times e^{j\phi_{M-1}}\mathcal{Z}$ , where  $e^{j\phi}\mathcal{Z} \triangleq \{e^{j\phi}z: z \in \mathcal{Z}\}$ , and  $\phi_0, \phi_1, \dots, \phi_{M-1}$  are the rotation angles to be specified. More precisely, signal sets  $S$  of the form  $S = \{\mathcal{F}_M(\Phi \underline{x}): \underline{x} \in \mathcal{Z}^M\}$ , where  $\Phi$  is an  $M$  by  $M$  diagonal matrix with the elements  $e^{j\phi_0}, e^{j\phi_1}, \dots, e^{j\phi_{M-1}}$  along the diagonal, will be considered. The largest magnitude at the output of an  $M$ -point IFFT will be equal to the largest magnitude of a signal in  $\mathcal{Z}$ , but now the elements of  $\Phi$  can be chosen to maximize  $d_{P,\min}(S)$ .

#### D. Rotation Angles for Specific Signal Sets

For a fixed  $M$  and  $\mathcal{Z}$ , the proposed construction immediately upper bounds  $d_{P,\min}(S)$  by  $d_{P,\min}^*$ , where

$$d_{P,\min}^* = \left( \frac{d_{E,\min}(\mathcal{Z})}{\sqrt{M}} \right)^M \quad (1)$$

and  $d_{E,\min}(\mathcal{Z}) = \min_{z_i, z_j \in \mathcal{Z}, i \neq j} |z_i - z_j|$ . This upper bound is derived in a straightforward manner as follows. Consider distinct vectors  $\underline{z}_i$  and  $\underline{z}_j$  in  $\mathcal{Z}^M$  that differ in only one complex dimension and whose separation in that dimension is the minimum Euclidean distance of the signal set  $\mathcal{Z}$ . Then, the Euclidean distance between these vectors is given by  $d_{E,\min}(\mathcal{Z})$ . Since multiplication of each of these signal vectors by the rotation matrix  $\Phi$  and the energy-preserving discrete Fourier transform operator preserves the Euclidean distance between the vectors,  $\mathcal{F}_M(\Phi \underline{z}_i)$  and  $\mathcal{F}_M(\Phi \underline{z}_j)$  differ in Euclidean distance by  $d_{E,\min}(\mathcal{Z})$ . The product distance between any two vectors separated by a fixed Euclidean distance is maximized when the Euclidean distance is spread equally across all  $M$  dimensions, and thus the product distance between  $\mathcal{F}_M(\Phi \underline{z}_i)$  and  $\mathcal{F}_M(\Phi \underline{z}_j)$  is at most  $d_{P,\min}^*$ .

The fact that  $d_{P,\min}(S)$  is upper bounded by  $d_{P,\min}^*$  is not overly discouraging if  $d_{P,\min}^*$  can be achieved, as (1) reveals that the distance between two signals of minimum Euclidean distance in  $S$  will be spread out across the full  $M$  complex dimensions equally, thus leading to the best pairwise error probability that can be obtained between two signals separated by this minimum Euclidean distance. It will be observed below that  $d_{P,\min}(S)$  will equal  $d_{P,\min}^*$  for nearly all signal sets  $S$  considered in this paper.

The analytic prescription of the optimal rotation matrix  $\Phi$  for various  $\mathcal{Z}$  and  $M$  has been found to be difficult; therefore, the rotation matrices presented in this section were found mainly by computer search. From these computer searches, it is apparent that, for  $J$ -ary PSK, a good selection for the matrix of rotation angles has diagonal elements given by  $\phi_i = 2\pi i/JM$  for  $i = 0, 1, \dots, M-1$ . For all of the BPSK and QPSK cases considered, such a selection results in a signal set  $S$  whose minimum product distance equals the upper bound (1). For 8-PSK, the minimum product distance of the resulting signal sets does not achieve the upper bound, but extensive computer search has not resulted in a better set of rotation angles. The best set of rotation angles found for a number of signal sets is given in Table I.

### III. APPLICATION

#### A. Uncoded Systems

A comparison of uncoded systems is not fair to the standard OFDM system, since it is well known that powerful coding must be employed in conjunction with OFDM on multipath fading channels for acceptable performance. Furthermore, the receiver complexity of the proposed system and that of a single-carrier system will exceed that of a standard OFDM system if no coding is allowed. However, in this section, brief numerical results are presented for a simple uncoded case to illustrate a few key points

TABLE I

BEST VECTOR OF ROTATION ANGLES  $(\phi_0, \phi_1, \dots, \phi_{M-1})$  FOR VARIOUS BASE SIGNAL SETS  $\mathcal{Z}$  AND COMPLEX DIMENSIONS  $M$ . IN EACH CASE, THE AVERAGE ENERGY PER COMPLEX DIMENSION IS NORMALIZED TO UNITY. NOTE THAT, WITH THE EXCEPTION OF THE 8-PSK SIGNAL SETS, ALL OF THE PROVIDED ROTATIONS RESULTS IN A SIGNAL SET  $S$  WHOSE MINIMUM PRODUCT DISTANCE  $d_{P,\min}(S)$  ACHIEVES THE UPPER BOUND  $d_{P,\min}^*$ . ONE SHOULD NOT ATTEMPT TO ASCERTAIN THE QUALITY OF A SIGNAL SET BY COMPARING THE PRODUCT DISTANCE ACROSS DIFFERENT  $M$ , SINCE THE TWO SYSTEMS UNDER COMPARISON WILL ACHIEVE DIFFERENT DIVERSITIES

$\mathcal{Z}$	$M$	$(\phi_0, \phi_1, \dots, \phi_{M-1})$	$d_{P,\min}(S)$	$d_{P,\min}^*$
BPSK	2	$(0, \frac{\pi}{2})$	2.0	2.0
	4	$(0, \frac{\pi}{4}, \frac{\pi}{2}, \frac{3\pi}{4})$	1.0	1.0
	8	$\phi_i = \frac{i\pi}{8}, i = 0, 1, \dots, 7$	0.0625	0.0625
	16	$\phi_i = \frac{i\pi}{16}, i = 0, 1, \dots, 15$	$1.53 \times 10^{-5}$	$1.53 \times 10^{-5}$
QPSK	2	$(0, \frac{\pi}{4})$	1.0	1.0
	4	$(0, \frac{\pi}{8}, \frac{\pi}{4}, \frac{3\pi}{8})$	0.25	0.25
	8	$\phi_i = \frac{i\pi}{16}, i = 0, 1, \dots, 7$	0.00391	0.00391
8-PSK	2	$(0, \frac{\pi}{8})$	0.233	0.293
	4	$(0, \frac{\pi}{16}, \frac{\pi}{8}, \frac{3\pi}{16})$	0.00368	0.0214
16-QAM	2	$(0, \frac{\pi}{4})$	0.20	0.20
	4	$(0, \frac{\pi}{8}, \frac{\pi}{4}, \frac{3\pi}{8})$	0.01	0.01
64-QAM	2	$(0, \frac{\pi}{4})$	0.0476	0.0476

about the proposed technique. Judgments on the utility of the technique should be reserved until coded results are considered in Section III-B.

In this paper, an uncoded system is defined to be one in which the *information* bits label the constellation points in  $S$ ; in other words, in an uncoded system, any sequence with symbols drawn from  $S$  is possible, whereas in a coded system the set of possible sequences is restricted. An OFDM symbol  $\underline{X}_k$  is formed at the transmitter per the recipe of Section II-B as follows. First,  $N/M$   $M$ -dimensional symbols  $\underline{u}_0, \dots, \underline{u}_{(N/M)-1}$  are formed, each by using  $\log_2 |S|$  bits output from the interleaver to select a symbol from  $S$ , where  $\underline{u}_l = (u_{l,0}, \dots, u_{l,M-1})^T$ . The elements of the OFDM symbol are then given by  $X_{k,l} = u_{l \bmod (N/M), \lfloor U(M/N) \rfloor}$ ,  $l = 0, 1, \dots, N-1$ . Although the aforementioned definitions give the precise mathematical definition of the system, note that the implementation of the transmitter can be simplified by recognizing that the proposed construction is forcing symbols at a given level of the IFFT in the OFDM transmitter to be drawn from a rotated version of the signal set  $\mathcal{Z}$ . Thus, in practice, the information bits to be carried on a given OFDM symbol could be used to directly select  $N/M$   $M$ -dimensional symbols from  $\{\Phi \underline{x} : \underline{x} \in \mathcal{Z}^M\}$  and then only the latter combining stages of the  $N$ -ary IFFT (roughly the complexity of  $M$   $N/M$ -point IFFTs—see Fig. 1) need be implemented to get the sample points for the OFDM symbol.

For all examples in this section, the two-path channel  $h(t) = h_0 \delta(t) + h_1 \delta(t - T_c)$  will be assumed, where  $\delta(t)$  is the Dirac delta function,  $T_c$  is the symbol period of the reference single-carrier system, and  $h_0$  and  $h_1$  are independent zero-mean complex Gaussian random variables of equal power. Perfect channel side information at the receiver is assumed for all cases. Assuming a signaling pulse in the single-carrier system that results in no ISI in the  $T_c$ -spaced samples of a matched filter output on an unfaded additive white Gaussian noise (AWGN) channel, a

whitened matched filter sampled at  $T_c$  intervals at the front end of the receiver will lead to the equivalent discrete-time channel  $h_0 + h_1 D$ , where  $D$  represents a one-symbol delay. Recognizing that the frequency separation of subchannels in an analogous OFDM system with  $N$  subcarriers is equal to  $1/NT_c$ , the correlation of the fading on subchannels  $i$  and  $j$  can be approximated as  $E[H_{k,i} H_{k,j}^*] = E[|h_0|^2] + E[|h_1|^2] e^{j2\pi(j-i)/N}$ ; thus, if attention is restricted to  $M = 2$ , the correlation is zero between the fading variables of the subchannels  $i$  and  $i + (N/2)$  of interest when  $E[|h_0|^2] = E[|h_1|^2]$  as assumed above. Thus, because  $H_{k,i}$  and  $H_{k,i+(N/2)}$  are jointly Gaussian, these two subchannels are faded independently. Although this seems a bit of fortuitous luck, the idea generalizes to more general channels and larger  $M$  in a natural way, as the  $M$  complex dimensions of the signal set  $S$  are spread across the full bandwidth equally and thus roughly capture the full diversity (up to  $M$ ) of the channel as expected. Note that the system designer does not need to know the statistics of the channel; if the channel has frequency diversity greater than or equal to  $M$  available, the system will capture diversity  $M$ , whereas if the system has frequency diversity less than  $M$  available, the system will capture the full frequency diversity the channel has available. Thus, the value of  $M$  does not need to be closely tuned to the channel.

As an example, consider  $M = 2$  and  $\mathcal{Z} = \text{QPSK}$ , which implies that the system will send two information bits per complex dimension. The settings  $\phi_0 = 0$  and  $\phi_1 = \pi/4$  result in  $d_{P,\min}(S) = d_{P,\min}^*$  for this example per Table I. Simulation results are shown in Fig. 2, where the proposed system has employed maximum-likelihood decoding for each uncoded symbol; note that the proposed system does indeed exhibit diversity two, as identified by the slope of its performance curve at high SNRs, but that it performs worse than a single-carrier system employing a maximum-likelihood sequence estimator (MLSE) for equalization. The fact that it performs worse than the MLSE-equalized single-carrier system was not guaranteed *a priori*, as the transmitted signal in the two systems is different. In fact, for the trivial (and somewhat unfair) example of  $M = 2$  and  $\mathcal{Z} = \text{BPSK}$ , the proposed system can achieve the matched filter bound and thus outperforms the MLSE-equalized single-carrier system. Finally, it is illustrative to contrast the proposed system with a frequency-domain equalized single-carrier system as proposed in [14]. In particular, the transmitted signals in the two systems are different, and, like a standard OFDM system, the proposed system allows a simple implementation of the optimal (nonlinear) receiver, which is in contrast to the linear receiver suggested in [14]. The resulting performance differences are apparent from Fig. 2.

### B. Coded Systems

In this section, simulation results for coded systems employing the proposed signal sets are presented. The goal is to maximize performance, which will be defined by the average SNR required to achieve a given error rate, while minimizing receiver complexity and the PMEPR of the system. After the system architecture for a coded system employing the proposed signal sets is detailed in Section III-B1, numerical results for

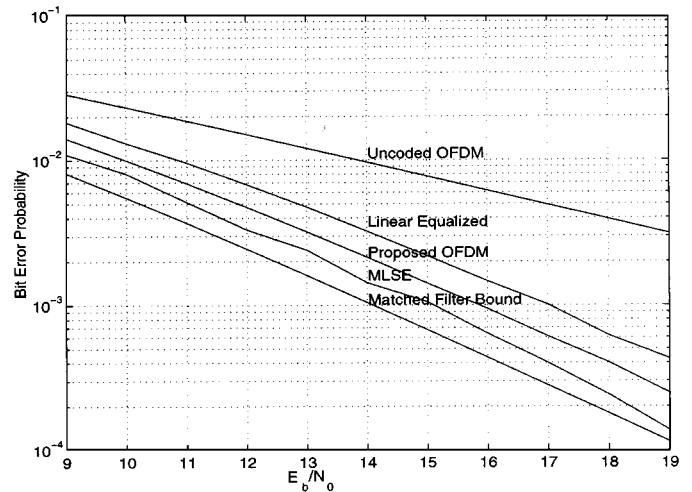


Fig. 2. Bit error probability of “uncoded” systems versus *average* SNR  $E_b/N_0$  per information bit on a Rayleigh fading channel with two paths of equal power spaced by the symbol period of the single-carrier system. The curve for the linear-equalized system approximates the performance of the “spread-spectrum multitone” and frequency-domain equalized systems of [7] and [14], respectively. The proposed system employs  $\mathcal{Z} = \text{QPSK}$  and  $M = 2$ . The number of trials was at least the product of 100 and the inverse of the bit error probability. For the MLSE curve, at least 10000 independent channels were simulated for each point.

the proposed architecture with optimal bit metric generation are presented in Section III-B2. These results suggest a moderate gain in performance in terms of *average* SNR for the proposed system over a standard OFDM system. A careful look at the complexity of metric generation in the proposed system motivates a slightly suboptimal receiver, which is presented along with the associated numerical results in Section III-B3; these results suggest that the proposed system can present an attractive alternative to a standard OFDM system from a performance versus complexity standpoint in terms of average SNR. Gains in PMEPR reduction of the proposed system, which also apply to an uncoded system, are reserved for Section IV.

1) *Coded System Architecture:* In this section, the architecture for coded systems that employ bit-interleaved coded modulation [15], [16] in conjunction with the proposed signal sets is introduced. As shown in Fig. 3, the formation of the coded input sequence  $\underline{X}_k$  is performed as follows. The sequence of information bits is coded with a convolutional code of maximal free distance. The resulting coded bits are interleaved. At the output of the interleaver, each OFDM symbol is formed as in the uncoded case. First,  $N/M$   $M$ -dimensional symbols  $\underline{u}_0, \dots, \underline{u}_{(N/M)-1}$  are formed, each by using  $\log_2 |S|$  bits output from the interleaver to select a symbol from  $S$ , where  $\underline{u}_l = (u_{l,0}, \dots, u_{l,M-1})^T$ . The elements of the OFDM symbol are then given by  $X_{k,l} = u_{l \bmod (N/M), \lfloor l(M/N) \rfloor}$ ,  $l = 0, 1, \dots, N - 1$ .

The constellation labeling, which defines the mapping of  $\log_2 |S|$  coded bits to a symbol in  $S$ , is a critical issue. In [16], Gray labeling is shown to possess a number of optimality properties for BICM schemes. Although the equivalent channel model between the encoder and the decoder for the proposed system is slightly different than that of [16] in the sense that different complex dimensions of the symbol are faded

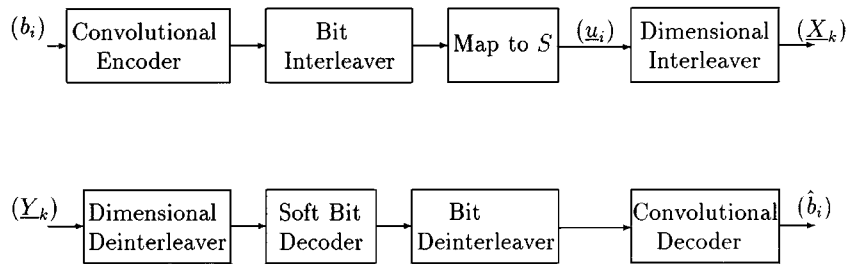


Fig. 3. Block diagrams for the baseband portions of the proposed BICM system. In the transmitter, the information bit sequence  $(b_i)$  is encoded with a convolutional code, and the resulting coded bits are interleaved at the bit level. At the output of the bit interleaver, the bits are mapped onto  $M$ -dimensional symbols from  $S$ . As in the uncoded case, the  $M$ -dimensional symbols  $\{u_i\}$  are taken  $N/M$  at a time and interleaved to form an OFDM symbol  $x_k$ . At the receiver, after the deinterleaving from the OFDM symbol to the  $M$ -dimensional symbols, the  $M$ -dimensional symbols are employed by the soft bit decoder to generate soft information on the coded bits. This soft information is then deinterleaved at the bit level before being employed by the convolutional decoder to decode the information bits.

independently, Gray labeling will be employed throughout this paper. As in [16], a signal set will be said to be Gray-labeled if any two signal points separated by the minimum Euclidean distance of the signal set have labels that differ in only a single bit location. Recognizing that rotating all signals in a signal set by a rotation  $\Phi$  does not alter the Euclidean distance between two signals in the signal set, a Gray-labeled signal set can be found by Gray labeling the signal points in  $\mathcal{Z}^M$  and then applying the rotation  $\Phi$ . Although Gray labeling seems like a reasonable choice, it should be noted that there is no proven optimality of such a labeling.

At the receiver, the bit deinterleaver in the receiver precludes optimal joint equalization/decoding. Instead, a soft-output bit decoder is employed before the bit deinterleaver as shown in Fig. 3, which generates the bit metrics for each of the  $\log_2 |S|$  bit locations in a received signal. This soft information is then deinterleaved and used by a Viterbi decoder to decode the information bits.

2) *Numerical Results Using Optimal Bit Metric Generation:* For simulation purposes, it is convenient to employ an equivalent discrete-time frequency-nonselective fading channel model for either the proposed or standard OFDM system operating over a frequency-selective fading channel. Let the proposed OFDM system operate with an  $M$ -dimensional signal set  $S$  derived from the one-dimensional (1-D) signal set  $\mathcal{Z}$  as specified above. On each corresponding set of  $M$  subcarriers, an analogous standard OFDM system will operate with an  $M$ -dimensional signal set  $S_{\text{OFDM}} = \mathcal{Z}^M$ . Then, assuming coherent detection with perfect timing, frequency, and phase recovery, an appropriate discrete-time frequency nonselective fading model is given by:  $r_{k,l} = \alpha_{k,l} s_{k,l} + n_{k,l}$ , where  $r_{k,l}$ ,  $k = -\infty, \dots, -1, 0, 1, \dots, \infty$ ,  $l = 0, 1, \dots, M-1$ , is the received signal corresponding to  $s_{k,l}$ , which is the  $l$ th dimension of the  $k$ th transmitted  $M$ -dimensional symbol from  $S$  or  $S_{\text{OFDM}}$ , and is faded by the Rayleigh random variable  $\alpha_{k,l}$ . The 2-D sequence  $n_{k,l}$  consists of zero-mean Gaussian random variables with  $E[|n_{k,l}|^2] = N_0$  that are i.i.d. in both dimensions. In this section, numerical results are obtained assuming optimal bit metric generation per [16] for the bit-interleaved coded modulation (BICM) decoder; that is, let  $b \in \{0, 1\}$  be the bit of interest and  $i \in \{0, 1, \dots, M \log_2 |\mathcal{Z}| - 1\}$ , be its position in the label of signals in  $S$ . Define  $\chi_b^i$  to be the set of

signal points in  $S$  such that the  $i$ th label position is equal to  $b$ . Then, per [16], the optimal metric increment to a branch metric for a trellis decoder for the hypothesized bit  $b$  in the  $i$ th label position is given by

$$\lambda_b^i(\underline{r}_k) = \log \sum_{\underline{x} \in \chi_b^i} \exp\left(-\frac{(|\underline{r}_k - \mathcal{A}_k \underline{x}|^2)}{N_0}\right) \quad (2)$$

where  $\underline{r}_k = (r_{k,0}, r_{k,1}, \dots, r_{k,M-1})^T$ , and  $\mathcal{A}_k$  is an  $M$  by  $M$  diagonal matrix with  $\alpha_{k,0}, \alpha_{k,1}, \dots, \alpha_{k,M-1}$  as its diagonal elements. In Section III-B3, the complexity of this metric generation will motivate a method of suboptimal metric generation.

For the numerical results, it will first be assumed that the system is operating in a fading environment that is rich in diversity, and thus the sequence  $\alpha_{i,l}$  is assumed to be a two-dimensional sequence of Rayleigh random variables that are i.i.d. in both dimensions. This corresponds to a system with at least  $M$ -ary frequency diversity available and either: 1) enough time diversity so that perfect interleaving of the coded bits in time can be assumed or 2) enough frequency diversity that perfect interleaving of the coded bits in the frequency domain can be assumed. The latter situation can occur in many wideband multicarrier environments, such as those commonly observed in fading environments for digital broadcast television [17].

For  $\mathcal{Z} = \text{QPSK}$  with  $M = 2$  and  $M = 4$ , simulation results are shown in Figs. 5 and 6, for various code complexities as a function of *average* received SNR. For comparison, the simulated performance of a standard OFDM system employing QPSK is shown in Fig. 4. In each case, rate-1/2 codes of maximum free distance obtained from [19, p. 330] are employed. Note that there is a moderate gain in performance versus average SNR for the proposed system. Recalling that all three systems exhibit the same Euclidean distance structure, this gain is attributed to the increased diversity of the proposed system.

As one would expect, the gain of the proposed system decreases if the total diversity (time and frequency) of the environment is limited. This issue is taken up in [20] by assuming that perfect interleaving of the coded bits is still obtained by both the standard and proposed OFDM schemes, but that the frequency diversity of the environment is limited to less than  $M$ , thereby implying correlation of the fading affecting the  $M$  subcarriers

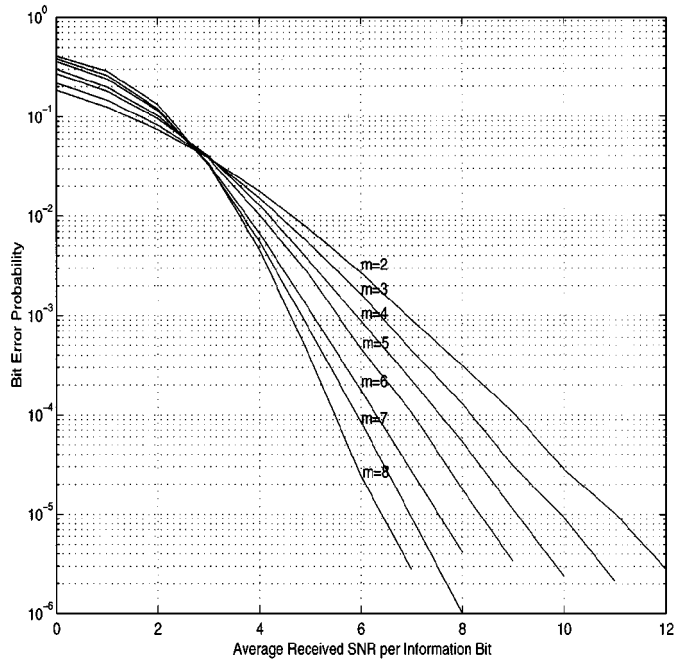


Fig. 4. Simulated bit error probability versus *average* received SNR  $E_b/N_0$  per information bit for a standard OFDM system employing BICM with a rate-1/2 code with memory  $m$  and QPSK signal sets on a Rayleigh fading channel. Perfect interleaving of the coded bits is assumed. Note the numerical evaluation of very tight exact union bounds is possible for this system [18], but simulation results are shown to facilitate a fair comparison to the simulation results of the proposed system. At least ten error events were observed for each simulation point.

that carry the  $M$  dimensions of a signal drawn from  $S$  for the proposed system. As the correlation increases, performance of the proposed system degrades to the performance of the standard OFDM system as expected [20].

3) *Complexity Analysis and a Suboptimal Receiver*: Whereas the results of Section III-B-2 suggest that the proposed system can perform better than a standard OFDM system in terms of required average signal-to-noise ratio to achieve a given error rate for the same number of trellis states in the decoder, receiver complexity needs to be carefully considered. In particular, for a standard OFDM system, a given position in a signal label impacts only one (complex) dimension of the  $M$  dimensions of the signal set  $S_{\text{OFDM}} = \mathcal{Z}^M$ , which greatly simplifies the metric generation process in (2) by reducing the size of the sets  $\chi_i^b$  that must be considered. This suggests that the complexity of the metric generation process must be studied carefully before conclusions are drawn.

Rather than study the complexity of the various systems employing (2), instead the suboptimal BICM metric calculation method of [16], which provides a better performance versus complexity tradeoff as demonstrated below, will be considered for the proposed signal sets. In particular, the suboptimal metric increment to a branch metric for the hypothesized bit  $b$  in the  $i$ th label position is given by

$$\tilde{\lambda}_b^i(\mathcal{L}_k) = -\log \min_{\mathcal{X} \in \chi_i^b} |\mathcal{L}_k - \mathcal{A}_k \mathcal{X}|^2. \quad (3)$$

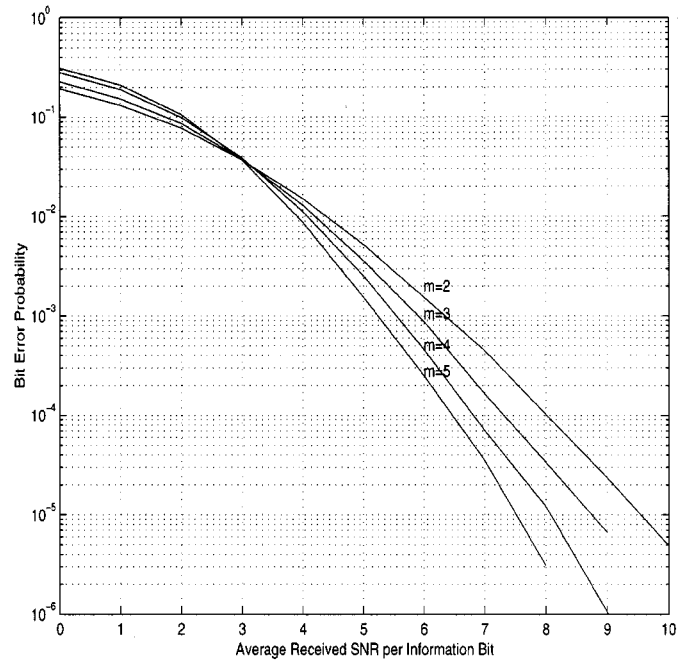


Fig. 5. Simulated bit error probability versus *average* received SNR  $E_b/N_0$  per information bit of the proposed OFDM system employing BICM with a rate-1/2 code with memory  $m$ , base signal set  $\mathcal{Z} = \text{QPSK}$ , and signal set dimension  $M = 2$  on a Rayleigh fading channel. Perfect interleaving of the coded bits and a channel frequency diversity of at least  $M$  is assumed. Optimal bit metric generation is assumed at the receiver. At least ten error events were observed for each simulation point.

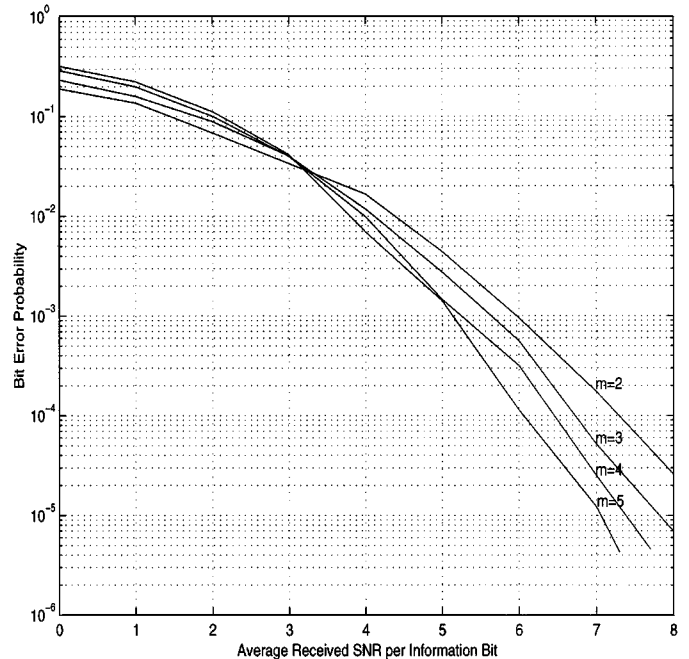


Fig. 6. Simulated bit error probability versus *average* received SNR  $E_b/N_0$  per information bit of the proposed OFDM system employing BICM with a rate-1/2 code with memory  $m$ , base signal set  $\mathcal{Z} = \text{QPSK}$ , and signal set dimension  $M = 4$  on a Rayleigh fading channel. Perfect interleaving of the coded bits and a channel frequency diversity of at least  $M$  is assumed. Optimal bit metric generation is assumed at the receiver. At least ten error events were observed for each simulation point.

Thus, under this suboptimal metric, only the Euclidean distance to the nearest signal in  $S$  that contains the hypothesized bit  $b$  at

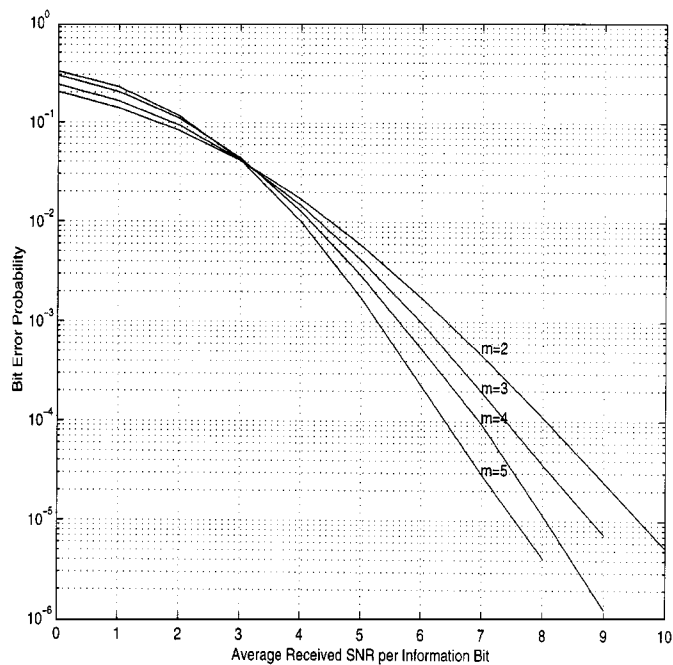


Fig. 7. Simulated bit error probability versus *average* received SNR  $E_b/N_0$  per information bit of the proposed OFDM system employing BICM with a rate-1/2 code with memory  $m$ , base signal set  $\mathcal{Z} = \text{QPSK}$ , and signal set dimension  $M = 2$  on a Rayleigh fading channel. Perfect interleaving of the coded bits and a channel frequency diversity of at least  $M$  is assumed. The suboptimal bit metric generation process presented in Section III-B-3 is assumed at the receiver. Note that there is almost no loss versus the system that employs optimal bit metric generation, particularly at high SNRs. At least ten error events were observed for each simulation point.

position  $i$  must be calculated. Using this suboptimal metric for the proposed system with  $\mathcal{Z} = \text{QPSK}$  and  $M = 2$ , the results shown in Fig. 7 are obtained. Note that there is almost no performance loss for a system employing the suboptimal metric of (3) versus a system that employs the optimal metric of (2).

Next, receiver complexity is considered for the standard OFDM and proposed OFDM systems employing the suboptimal metric of (3). This complexity analysis is presented in detail for the case of  $\mathcal{Z} = \text{QPSK}$  and  $M = 2$  to demonstrate a few key points. First, consider the standard OFDM system. For  $\mathcal{Z} = \text{QPSK}$  in the standard OFDM system, the system operates as a standard coded QPSK system rather than a true BICM system; thus, the suboptimal metric of (3) can be shown to be optimal, and, it can be easily shown that only a single multiply with real operands is required to generate the metrics for a received channel bit. Recall that this is one of the key motivations for a standard OFDM system, since this greatly reduces the number of multipliers required in equalization and decoding versus those required in the feedforward portion of a decision-feedback equalizer.

Next, consider the proposed system with  $\mathcal{Z} = \text{QPSK}$  and  $M = 2$ , employing the metric generation of (3). By observing the signal set (see Fig. 8), it can be shown that the number of multipliers required to calculate the Euclidean distance between the received symbol and each signal point can be greatly simplified due to the structure of the signal set. For a given received  $M$ -dimensional symbol  $\underline{r}_k$ , employment of the suboptimal metric requires that the closest signal in  $\chi_i^0$  and  $\chi_i^1$  to  $\underline{r}_k$

be found for each  $i = 0, 1, 2, 3$ . This requires the calculation of the Euclidean distance squared

$$\begin{aligned} d_E^2(\underline{r}_k, \underline{s}) &= |\underline{r}_k - \mathcal{A}_k \underline{s}|^2 \\ &= |\underline{r}_k|^2 - 2\text{Re}(\underline{r}_k^H \mathcal{A}_k \underline{s}) + \underline{s}^H \mathcal{A}_k \mathcal{A}_k \underline{s} \end{aligned}$$

for all  $\underline{s} \in S$ . Recognizing that the first term is common to all branches, it need not be computed. Using the fact that there are only two possible magnitudes for each of the dimensions of the vectors drawn from  $S$ , the last term can be computed for all  $\underline{s} \in S$  with six multipliers with real operands. Likewise, exploiting the fact that there are only three possible values for each real dimension of a signal  $\underline{s} \in S$ , the second term can be computed for all  $\underline{s} \in S$  with only sixteen real multipliers. Thus, the calculation of the Euclidean distances for all  $\underline{s} \in S$  requires 22 multiplies with real operands, or 11 multipliers with real operands per complex dimension.

Depending on the number of subcarriers employed and the method of performing channel estimation (e.g., see [21]) in a coherent OFDM receiver, the complexity of metric generation is not likely to add significant complexity to the OFDM receiver. However, consider the comparison of the proposed system with a standard OFDM system based on just the complexity of the metric generation and the trellis decoding. The complexity of the metric generation for the proposed system does not grow, of course, with an increasing number of states in the trellis decoder. Thus, observing from Figs. 4 and 5 that for  $\mathcal{Z} = \text{QPSK}$  and  $M = 2$  the proposed system requires two to four times less states in its trellis decoder than the standard OFDM system for the same performance, it will likely yield a lower complexity receiver for high-performance systems with a large number of states in the trellis (for example, 32 states in the proposed system versus 64–128 states in the standard OFDM system).

The proposed system can be viewed as allowing a small amount of controlled equalization in the system. For  $M = 2$ , the effectively frequency-nonselctive channels of the OFDM system are turned into effectively two-tap channels, regardless of the length of the true ISI channel. For example, on a fading channel with ISI extending over many tens of symbol periods, it may be difficult in many single-carrier systems to support the complexity of a feedforward filter in a decision-feedback equalizer with a sufficient number of taps for acceptable performance, which suggests employing an OFDM system. The proposed system would allow the system to act as a single-carrier system over a two-tap ISI channel in such cases, which may provide certain performance versus complexity tradeoff advantages per above.

#### IV. PMEPR CHARACTERIZATION

As will be demonstrated below, the proposed system will provide modest improvements in the system PMEPR versus a standard OFDM system. Due to the importance of the PMEPR problem in OFDM systems, the application of the OFDM system architecture in broadcast applications, and the consideration of OFDM for future two-way low-power communications, there has been significant research work on

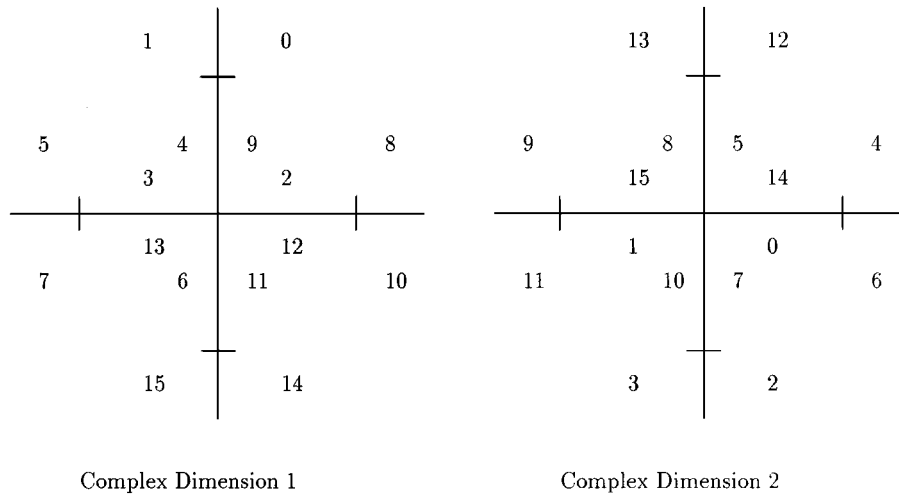


Fig. 8. The two complex dimensions for each signal in the proposed signal set for  $\mathcal{Z} = \text{QPSK}$  and  $M = 2$ . A number plotted on one of the two complex dimensions indicates the complex value for that dimension of the signal whose index is that number. To avoid confusion, the axes of the graphs are not labeled, but each tick mark indicates a distance of unity.

the reduction of the PMEPR in OFDM systems. This work can be roughly divided into two groups.

The first group consists of techniques that do not alter the coding and modulation, but instead manipulate the baseband transmitted waveform with some form of preprocessing/post-processing of the inverse fast Fourier transform (IFFT) inputs/outputs at the transmitter (e.g., selective mapping [22]–[24], partial transmit sequences [25], peak windowing [26], [27], convex projection [28], [29], or fixed phase rotation [30]). These techniques generally reduce the system PMEPR at the cost of a small complexity increase and/or a small decrease in system bandwidth efficiency. Many of these techniques have the potential to be employed in conjunction with the proposed scheme to effect significant PMEPR reductions for the OFDM system.

The second group of techniques exploit the fact that coding is a natural sequence restrictor and thus employ some form of coded modulation to restrict the sequences allowable across the input of the IFFT. Early work in this area consisted of computer searches for good codewords or the optimal coset of a given code (e.g., [31]). Recent work has focused on existing codes whose codewords do not exhibit peaks when the codewords are placed across the input of the IFFT; these techniques have converged to solutions that draw codewords from Golay complementary sequences [32], which have recently been recognized as cosets of first-order Reed–Muller codes [33]–[35]. However, the elegant results of this path of research may have limited utility; in particular, the codes are being specifically chosen for their PMEPR reduction capability at the expense of error control capability, as pointed out in [34]. In contrast, the coded modulation schemes proposed in this paper reduce the PMEPR of the OFDM system while improving the performance of powerful trellis coded modulation techniques in terms of bit error probability versus *average* SNR.

Consider the PMEPR characteristics of the proposed system for a given  $M$  and  $\mathcal{Z}$ . From the construction in Section II, it is clear that, for the same average transmitted energy in the proposed OFDM and standard OFDM system, the proposed system

achieves a reduction of  $10 \log_{10} M$  dB in the *maximum* squared magnitude of an output of the  $N$ -point IFFT at the transmitter. However, the maximum magnitude occurs very rarely in OFDM systems with reasonably large  $N$ , and thus this may not be the most pertinent measure of the system's PMEPR performance. Thus, the PMEPR properties of the proposed system must be characterized more carefully.

Let the PMEPR of symbol  $k$  be defined as the ratio of the maximum squared value of the signal envelope on  $(kT_s, (k+1)T_s)$  to the (ensemble) average transmitted energy  $E_s$  of the system

$$\zeta_k = \frac{1}{NE_s} \max_{0 \leq t \leq T_s} \left| \sum_{l=0}^{N-1} X_{k,l} \exp \left( j2\pi \frac{l - \frac{N}{2}}{T_s} t \right) \right|^2.$$

The PMEPR of various systems will be characterized by the cumulative distribution function of  $\zeta_k$ , which is given by  $F_{\zeta_k}(x) = P[\zeta_k \leq x]$ .

If the system PMEPR is calculated by only considering samples in the baseband transmitted waveform corresponding to the outputs  $x_{k,0}, x_{k,1}, \dots, x_{k,N-1}$  of the IFFT, it can be shown that significant PMEPR gains are obtained for the proposed OFDM system over the standard OFDM system. These gains are notable in that they correspond to a measure that is independent of the pulse shaping. However, to consider the PMEPR characterization of the system more carefully, the minimum bandwidth ISI-free pulse is employed [i.e.,  $\sin(\pi t/NT_s)/(\pi t/NT_s)$ ], the waveform is sampled at a much higher rate, and  $\zeta_k$  is calculated based on the resulting samples. For the proposed and standard OFDM systems, a typical example of the complement of the resulting distribution function is shown for  $\mathcal{Z} = \text{QPSK}$  and various  $M$  and  $N$  in Fig. 9. Note that the  $M = 1$  curve corresponds to a standard OFDM system. One can observe from Fig. 9 that, for a given  $N$ , only a modest (but not insignificant) improvement in the PMEPR characteristics of the system is obtained by employing the signal sets of Section II, particularly when the ratio  $N/M$  is small.

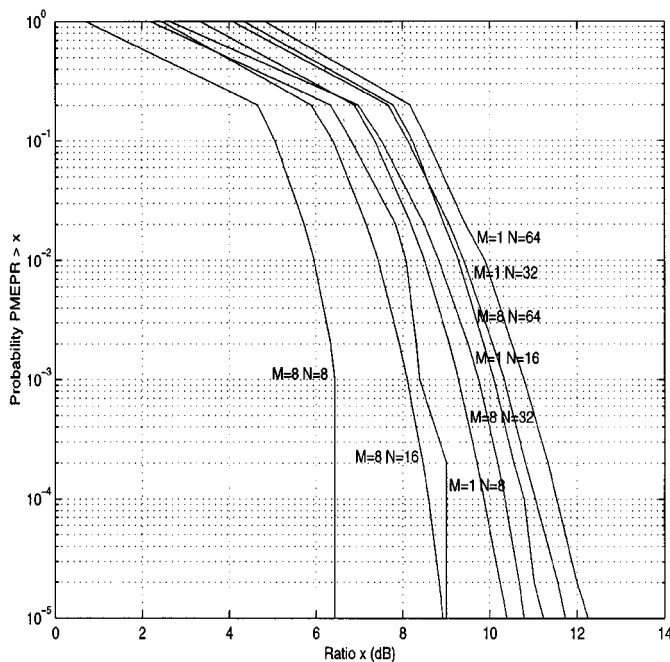


Fig. 9. The probability that the PMEPR of the baseband transmitted signal for a given OFDM symbol exceeds a given level for various numbers of subcarriers  $N$  and signal set dimensions  $M$  with  $\mathcal{Z} = \text{QPSK}$ . For this calculation, the baseband waveform has been sampled at least eight times between the locations of the IFFT outputs (often termed “oversampling by a factor of eight”). The number of OFDM symbols simulated for each curve is  $5 \times 10^5$ . Note that  $M = 1$  corresponds to a standard OFDM system whereas  $M = N$  corresponds to a standard single-carrier system.

## V. CONCLUSION

In this paper, a method of prescribing multidimensional signal sets for an OFDM system has been presented. At a small increase in the complexity of metric generation at the receiver, the signal sets can significantly increase the diversity of the coded modulation scheme, which leads to gains in the performance of the system as a function of the average SNR of the system. A suboptimal receiver has been described, and the characterization of its performance leads to the conclusion that, assuming perfect synchronization and channel estimation, the prescribed signal sets can provide an attractive performance versus complexity tradeoff alternative to standard OFDM for systems operating in environments rich in diversity. Furthermore, modest gains in the PMEPR of the system are obtained through a signal set design constraint which does not compromise the minimum product distance of the signal sets.

In the broader context, the proposed OFDM signal set construction can be viewed as effectively adding a small amount of controlled equalization into the system by introducing aspects of a single-carrier system into the multicarrier system. To illustrate this more clearly, note that the construction essentially guarantees that standard signal sets (e.g., BPSK, QPSK) occur in the IFFT decomposition at deeper levels as  $M$  increases. In the limit when  $M = N$ , the resulting system is indeed a single-carrier system operating on a wideband wireless channel with a number of redundant symbols equal to the length of the cyclic prefix. Thus, the proposed system can be viewed as a general framework that encompasses both multicarrier and

single-carrier systems. The choice of  $M$  defines the combination of the two systems that the proposed system is employing, with  $M = 1$  corresponding to a standard multicarrier system and  $M = N$  corresponding to a standard single-carrier system. Systems with small  $M$  have characteristics similar to OFDM systems and thus tend to demonstrate less diversity for a given code, worse PMEPR characteristics, and simpler metric generation, whereas systems with large  $M$  are more similar to single-carrier systems and thus tend to demonstrate more diversity for a given code, better PMEPR characteristics, and more complicated metric generation. Note that the diversity (and thus performance) obtained by the proposed single-carrier/multicarrier hybrid is higher than that obtained if one considers the most straightforward hybrid:  $N/M$  single-carrier systems, each occupying a fraction  $M/N$  of the bandwidth.

It is also apparent directly from the construction that the choice of  $M$  in a coded system also indicates the proper combination of bit-interleaved coded modulation [16] and lattice techniques [10] for the operation of perfectly-interleaved coded modulation schemes operating over frequency-nonselective fading channels. Note that this implies that, from a coding, modulation, and equalization perspective, the question of the proper combination of single-carrier and multicarrier systems is equivalent to the question of what is the proper combination of BICM and lattice techniques for systems achieving perfect interleaving on frequency-nonselective fading channels.

Finally, as in previous work with rotated signal sets followed by interleaving of the various dimensions [38], it should be noted that the effect of imperfect channel estimation can have a significant impact on the comparison of such schemes to those employing standard nonrotated signal sets; in particular, the performance degradation when imperfect channel estimates are available is generally greater for the rotated signal sets. Thus, the question of the proper combination of multicarrier and single-carrier systems under imperfect channel estimation remains an important topic for future work.

## REFERENCES

- [1] M. Tomlinson, “New automatic equalizer employing modulo arithmetic,” *Electron. Lett.*, vol. 7, pp. 138–139, Mar. 1971.
- [2] H. Harashima and H. Miyakawa, “Matched-transmission technique for channels with intersymbol interference,” *IEEE Trans. Commun.*, vol. COM-20, pp. 774–780, Aug. 1972.
- [3] I. Kalet, “The multitone channel,” *IEEE Trans. Commun.*, vol. 37, pp. 119–124, Feb. 1989.
- [4] D. Goeckel, “Adaptive coding for time-varying channels using outdated fading estimates,” *IEEE Trans. Commun.*, vol. 47, pp. 844–855, June 1999.
- [5] C. Douillard, M. Jezequel, C. Berrou, A. Picart, P. Didier, and A. Glavieux, “Iterative correction of intersymbol interference: Turbo-equalization,” *Eur. Trans. Telecommun.*, vol. 6, pp. 507–511, Sept.–Oct. 1995.
- [6] A. Anastasopoulos and K. Chugg, “TCM for frequency-selective, interleaved fading channels using joint diversity combining,” in *Proc. 1998 Int. Conf. Communications*, June 1998, pp. 1340–1344.
- [7] S. Wilson, “Digital audio broadcasting in a fading and dispersive channel,” Ph.D. dissertation, Stanford University, Stanford, CA, Aug. 1994.
- [8] L. Cimini, Jr., “Performance studies for high-speed indoor wireless communications,” *Wireless Personal Commun.*, vol. 2, pp. 67–85, 1995.
- [9] K. Boule and J. C. Belfiore, “Modulation schemes designed for the Rayleigh channel,” in *Proc. Conf. Information Sciences and Systems*, 1992, pp. 288–293.

- [10] J. Boutros and E. Viterbo, "Signal space diversity: A power- and bandwidth-efficient diversity technique for the Rayleigh fading channel," *IEEE Trans. Inform. Theory*, pp. 1453–1467, July 1998.
- [11] A. Ruiz, J. Cioffi, and S. Kasturia, "Discrete multiple tone modulation with coset coding for the spectrally shaped channel," *IEEE Trans. Commun.*, vol. 40, pp. 1012–1029, June 1992.
- [12] P. Bello, "Characterization of randomly time-variant linear channels," *IEEE Trans. Commun. Syst.*, vol. 11, pp. 360–393, Dec. 1963.
- [13] J. Proakis, *Digital Communications: Third Edition*. New York: McGraw-Hill, 1995.
- [14] H. Sari, G. Karam, and I. Jeanclaude, "Transmission techniques for digital terrestrial TV broadcasting," *IEEE Commun. Mag.*, pp. 100–109, February 1995.
- [15] E. Zehavi, "8-PSK trellis codes for a Rayleigh channel," *IEEE Trans. Commun.*, vol. 40, pp. 873–884, May 1992.
- [16] G. Caire, G. Taricco, and E. Biglieri, "Bit-interleaved coded modulation," *IEEE Trans. Inform. Theory*, vol. 44, pp. 927–946, May 1998.
- [17] G. Huffard, "A characterization of the multipath in the HDTV channel," *IEEE Trans. Broadcast.*, vol. 38, pp. 252–255, Dec. 1992.
- [18] M. Simon and D. Divsalar, "Some new twists to problems involving the Gaussian probability integral," *IEEE Trans. Commun.*, vol. 46, pp. 200–210, Feb. 1998.
- [19] S. Lin and D. Costello, Jr., *Error Control Coding: Fundamentals and Applications*. Englewood Cliffs, NJ: Prentice-Hall, 1983.
- [20] D. Goeckel and G. Ananthaswamy, "Increasing diversity with non-standard signal sets in wireless OFDM systems," in *Proc. 1999 IEEE Wireless Communications and Networking Conf.*, September 1999, pp. 20–24.
- [21] Y. Li, L. Cimini, Jr., and N. Sollenberger, "Robust channel estimation for OFDM systems with rapid dispersive fading channels," *IEEE Trans. Commun.*, vol. 46, pp. 902–915, July 1998.
- [22] D. Mestdagh and P. Spruyt, "A method to reduce the probability of clipping in DMT-based transceivers," *IEEE Trans. Commun.*, vol. 44, pp. 1234–1238, Oct. 1996.
- [23] R. Bäuml, R. Fischer, and J. Huber, "Reducing the peak-to-average power ratio of multicarrier modulation by selected mapping," *Electron. Lett.*, vol. 32, pp. 2056–2057, Oct. 1996.
- [24] P. Van Eetvelt, G. Wade, and M. Tomlinson, "Peak to average power reduction for OFDM schemes by selective scrambling," *Electron. Lett.*, vol. 32, pp. 1963–1964, Oct. 1996.
- [25] S. Müller and J. Huber, "OFDM with reduced peak-to-average power ratio by optimum combination of partial transmit sequences," *Electron. Letters*, vol. 33, pp. 368–369, Feb. 1997.
- [26] M. Pauli and H. Kuchenbecker, "Minimization of the intermodulation distortion of a nonlinearly amplified OFDM signal," in *Wireless Personal Communications 4*. Boston, MA: Kluwer, 1997.
- [27] R. van Nee and A. Wild, "Reducing the peak-to-average power ratio of OFDM," in *Proc. 48th IEEE Vehicular Technology Conf.*, 1998, pp. 2072–2076.
- [28] A. Gatherer and M. Polley, "Controlled clipping probability in DMT transmission," in *Proc. 1997 Asilomar Conf. Signals, Systems, and Computers*, 1997.
- [29] J. Tellado and J. Cioffi, "Peak power reduction for multicarrier transmission," in *Proc. 1998 Global Communications Conf.*, 1998.
- [30] V. Tarokh and H. Jafarkhani, "On the computation and reduction of the peak-to-average power ratio in multicarrier communications," *IEEE Trans. Commun.*, vol. 48, pp. 37–44, Jan. 2000.
- [31] A. Jones, T. Wilkinson, and S. Barton, "Block coding scheme for the reduction of peak to mean envelope power ratio of multicarrier transmission schemes," *Electron. Lett.*, vol. 30, pp. 2098–2099, Dec. 1994.
- [32] R. van Nee, "OFDM codes for peak-to-average power reduction and error correction," in *Proc. 1996 Global Communications Conf.*, 1996, pp. 740–744.
- [33] A. Grant and R. van Nee, "Efficient maximum likelihood decoding of peak power limiting codes for OFDM," in *Proc. 48th IEEE Vehicular Technology Conf.*, 1998, pp. 2081–2084.
- [34] A. Jones and T. Wilkinson, "Performance of Reed–Muller codes and a maximum-likelihood decoding algorithm for OFDM," *IEEE Trans. Commun.*, pp. 949–952, July 1999.
- [35] J. Davis and J. Jedwab, "Peak-to-mean power control in OFDM, Golay complementary sequences, and Reed–Muller codes," *IEEE Trans. Inform. Theory*, vol. 45, pp. 2397–2417, Nov. 1999.
- [36] U. Fincke and M. Pohst, "Improved methods for calculating vectors of short length in a lattice, including a complexity analysis," *Mathematics of Computation*, vol. 44, pp. 463–471, Apr. 1985.
- [37] E. Viterbo and J. Boutros, "A universal lattice decoder for fading channels," *IEEE Trans. Inform. Theory*, vol. 45, pp. 1639–1642, July 1999.
- [38] B. Jeličić and S. Roy, "Design of trellis coded QAM for flat fading and AWGN channels," *IEEE Trans. Veh. Technol.*, vol. 44, pp. 192–201, Feb. 1995.



**Dennis L. Goeckel** received the B.S.E.E. degree from Purdue University, West Lafayette, IN, in 1992 and the M.S.E.E. and Ph.D. degrees, both in electrical engineering, from the University of Michigan, Ann Arbor, in 1993 and 1996, respectively.

From 1987 to 1992, he worked at Sundstrand Corporation. From 1992 to 1996, he was a National Science Foundation Graduate Fellow at the University of Michigan. In September 1996, he assumed his current position as an Assistant Professor with the Electrical and Computer Engineering Department, University of Massachusetts, Amherst. In September 1996, he assumed his current position as an Assistant Professor with the Electrical and Computer Engineering Department, University of Massachusetts, Amherst, where he is currently an Associate Professor.

Dr. Goeckel is the recipient of a 1999 CAREER Award from the National Science Foundation. Currently, he is an Editor for the IEEE TRANSACTIONS ON WIRELESS COMMUNICATIONS.



**Ganesh Ananthaswamy** received the M.Tech. degree in communication engineering from the Indian Institute of Technology, Bombay, India in 1996 and the Ph.D. in electrical engineering from the University of Massachusetts, Amherst, in 2001.

He is currently a System Design Engineer with Analog Devices, Inc., Wilmington, MA, working on the design and development of a broad-band wireless modem conforming to the BWIF specifications. His current research interests include channel estimation and synchronization algorithms for OFDM systems, channel modeling, and wavelet transforms.